

August 1, 1998

SPIN@FERMI PROPOSAL

to

Fermilab

Analyzing power A_n in 120 GeV high- P_{\perp}^2
proton-proton elastic scattering

by

SPIN@FERMI Collaboration:

Michigan, Virginia, IHEP-Protvino,
JINR-Dubna, INR-Troitsk, TRIUMF

Table of Contents

SPIN@FERMI Collaboration Participants	p. 2
Introduction	p. 3
Theoretical Background	p. 4
Polarized Proton Target	p. 6
Rastering and Beam Stability Requirements	p. 8
Recoil and Forward Spectrometers	p. 10
Event Rates	p. 15
Status of Equipment	p. 17
Summary	p. 18
References	p. 18

Introduction

This is a proposal to measure the analyzing power A_n in proton-proton elastic scattering at P_{\perp}^2 of 1 to 12 $(\text{GeV}/c)^2$ using a 120 GeV unpolarized extracted proton beam from Fermilab's Main Injector starting in 2001. We would scatter the high intensity beam from a transversely polarized proton target and measure the quantity,

$$A_n = \frac{A_{mea}}{P_T} = \frac{1}{P_T} \left[\frac{N(\uparrow) - N(\downarrow)}{N(\uparrow) + N(\downarrow)} \right], \quad (1)$$

where A_{mea} is the measured asymmetry, P_T is the target polarization, and $N(\uparrow)$ and $N(\downarrow)$ are the normalized elastic event rates with the target's spin direction up and down, respectively.

Our main goal is to determine if the unexpectedly large A_n value, discovered in large- P_{\perp}^2 proton-proton elastic scattering at the AGS, persists to higher energy and larger P_{\perp}^2 . At 24 GeV the one-spin analyzing power A_n was found ^[1,2] to be $20.4\% \pm 3.9\%$ near P_{\perp}^2 of 7 $(\text{GeV}/c)^2$, as shown in Fig. 1. This large and unexpected spin effect has been difficult to reconcile with conventional models of strong interactions such as perturbative Quantum Chromodynamics (QCD). Perturbative QCD's validity is predicted to improve with increasing energy and increasing P_{\perp}^2 . This proposed experiment would increase the maximum energy for high- P_{\perp}^2 A_n data from 28 to 120 GeV; it would also increase the maximum P_{\perp}^2 from 7 to 12 $(\text{GeV}/c)^2$.

The proposed experiment would use the Michigan 1-watt-cooling-power solid polarized proton target containing radiation-doped frozen ammonia (NH_3) beads. This target^[4] successfully operated with an average beam intensity of 10^{11} protons per sec at the AGS, allowing the precise large- P_{\perp}^2 measurements^[1] of A_n shown in Fig. 1.

This high-cooling-power polarized proton target, along with a high intensity extracted proton beam from the Main Injector of about $3 \cdot 10^{11}$ protons per 2.8 s cycle, would give a polarized proton luminosity of about $2 \cdot 10^{34} \text{ s}^{-1} \text{ cm}^{-2}$. This would allow precise measurements of the analyzing power A_n in large- P_{\perp}^2 proton-proton elastic scattering at 120 GeV out to a P_{\perp}^2 of about 12 $(\text{GeV}/c)^2$.

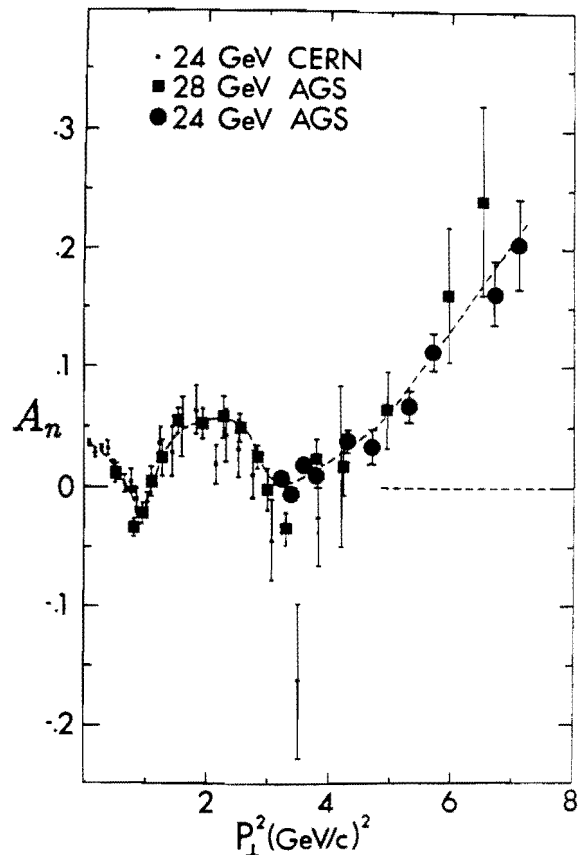


Fig. 1. The analyzing power A_n is plotted against P_{\perp}^2 for spin polarized proton-proton elastic scattering at 24^[1,3] and 28 GeV^[2].

We propose to run in the Meson West extracted beam area, which seems well suited for this high- P_{\perp}^2 elastic scattering experiment. We would use a 40-m-long recoil-arm spectrometer, similar to the NEPTUN-A spectrometer designed for UNK^[5], consisting of magnets with considerable bending power, medium-resolution scintillation hodoscopes, and high-resolution proportional and drift wire chambers. The resulting high-precision measurements of the recoil momentum and angle together with a simple forward arm containing only one hodoscope should allow a clear identification of elastic events. Focusing quadrupoles in the recoil spectrometer would reduce the angular divergence of the recoil protons and thus would significantly increase the angular acceptance and reduce the background. Moreover, rastering the extracted beam would allow determination of the interaction point's transverse position to a precision of ± 1.25 mm.

This proposal contains a brief discussion of the theoretical background of spin effects in large- P_{\perp}^2 elastic scattering; we next describe the Michigan polarized proton target, the beam requirements, and the proposed recoil and forward spectrometers. We then calculate the expected event rates and errors for the proposed SPIN@FERMI experiment, and review its equipment status.

Note that the 120 GeV Main Injector could later be given polarized beam capability, as described in the Fermilab-supported study *Acceleration of Polarized Protons to 120 GeV and 1 TeV at Fermilab*, SPIN Collaboration UM HE 95-09 (24 July 1995), at a total cost of about 8 Million 1995 Dollars. Our SPIN@FERMI experiment could then measure the elastic spin-spin parameter A_{nn} with excellent precision, as mentioned in Table 5.

Theoretical Background

Since the single-spin asymmetry A_n can be written as an interference between the spin flip and non-flip amplitudes, the dispersion theory requirement that all amplitudes with the same energy dependence have the same asymptotic phase implies that A_n should vanish at large s . At large P_{\perp}^2 , dynamical mechanisms involving individual constituents evade these constraints; thus, spin experiments on large- P_{\perp}^2 hadron elastic scattering can provide important information about the short range interactions of the hadron's constituents and about the hadronic wavefunctions.

According to the perturbative Quantum Chromodynamic (QCD) approach^[6], only the lowest Fock states with valence quarks and zero orbital angular momentum contribute to the elastic scattering. This approach leads to the power-law dimensional scaling quark-counting rule^[7]; its predictions for form factors and two-body hadron scattering cross-sections are generally consistent with unpolarized data at P_{\perp}^2 above a few $(\text{GeV}/c)^2$. However, this agreement with unpolarized data does not in itself confirm the validity of the perturbative QCD approach^[6]. The large spin effects found experimentally in $p + p \rightarrow p + p$ ^[8] demonstrate trends which challenge the perturbative QCD approach.^[9]

For the exclusive reaction $a+b \rightarrow c+d$, perturbative QCD gives a simple and general helicity conservation law^[6]

$$\lambda_a + \lambda_b = \lambda_c + \lambda_d, \quad (2)$$

where λ_i is the helicity of the i^{th} particle. This relation implies that the analyzing power A_n in elastic proton-proton scattering should vanish at large- P_{\perp}^2 :

$$|A_n| \leq \text{constant}/P_{\perp}. \quad (3)$$

Violation of this relation would demonstrate the possible non-perturbative nature of hadronic dynamics and/or the presence of states with non-zero orbital angular momentum^[10]. As shown in Fig. 1, the proton-proton elastic analyzing power data^[1,2,3] at 24 and 28 GeV clearly demonstrate that A_n is rising at the largest measured P_{\perp}^2 of 7 (GeV/c)² and there is no evidence for a $1/P_{\perp}$ falloff.

Large transverse spin effects have now been consistently observed in both elastic and inelastic high- P_{\perp}^2 experiments^[1-3,11-14]. In the framework of QCD, these spin effects are sensitive to non-perturbative dynamics due to chiral symmetry breaking or confinement effects. Several models have been proposed for the treatment of these large spin effects at high P_{\perp}^2 ^[15-27]. These models involve non-perturbative mechanisms such as: strange and charmed particle production thresholds^[18], geometric mechanisms of quark scattering in an effective field^[19] and quark interactions due to an infinite sequence of meson exchanges^[20]. Some of these models were able to reproduce the large values for the elastic spin-spin parameter A_{nn} observed at the ZGS^[11,12] near 12 GeV and $\theta_{\text{cm}} = 90^\circ$, as well as the 18.5 GeV AGS data on A_{nn} ^[28]. Some other models give an explanation for the large value of the analyzing power A_n discovered in high- P_{\perp}^2 elastic scattering^[1]. However, there is not yet a model that can simultaneously explain all the spin effects found in proton-proton elastic scattering^[1-3,11,12] and inelastic scattering^[13,14].

Our proposed study of elastic scattering spin effects in the totally unexplored region near $P_{\perp}^2 = 12$ (GeV/c)² should provide another test of perturbative QCD. It should also yield information about the hadronic interactions and wave functions which cannot be obtained from deep-inelastic scattering. It might also provide new insights into the mechanism of chiral symmetry breaking and quark helicity flip. Some of the above models predict large values for A_n at higher energies; for example, the quark U-matrix model^[19] predicts, for elastic proton-proton scattering at 120 GeV, an A_n of about 12% at $P_{\perp}^2 = 12$ (GeV/c)².^[29] Thus, it seems quite important to measure, at $P_{\perp}^2 = 12$ (GeV/c)² and 120 GeV, the $p-p$ elastic A_n and then later A_{nn} if polarized proton capability is added to the new Main Injector.

Polarized Proton Target

We propose to use the University of Michigan's 1-watt-cooling-power polarized proton target^[4] (PPT) which is shown in Fig. 2 and described in Table 1. The target material is radiation-doped ammonia (NH_3), formed into beads of about 2 mm, with a net hydrogen density of about 0.10 g cm^{-3} . The target's length is about 3.6 cm, and its diameter is about 2 cm. The proton polarization in the 5 T field is driven by a 140 GHz microwave system using the Dynamic Nuclear Polarization method. The polarization is monitored by a 213 MHz NMR Q-meter system. This target was successfully used at the AGS in 1990^[1,30]; at its magnetic field of 5 T and temperature of 1 K, it has an unexpectedly high proton polarization of up to 96%^[4]. Moreover, its 5 minute polarization rise-time allows fast and frequent target polarization-direction reversals. The high polarization and short polarization growth-time are clearly shown in Fig. 3.

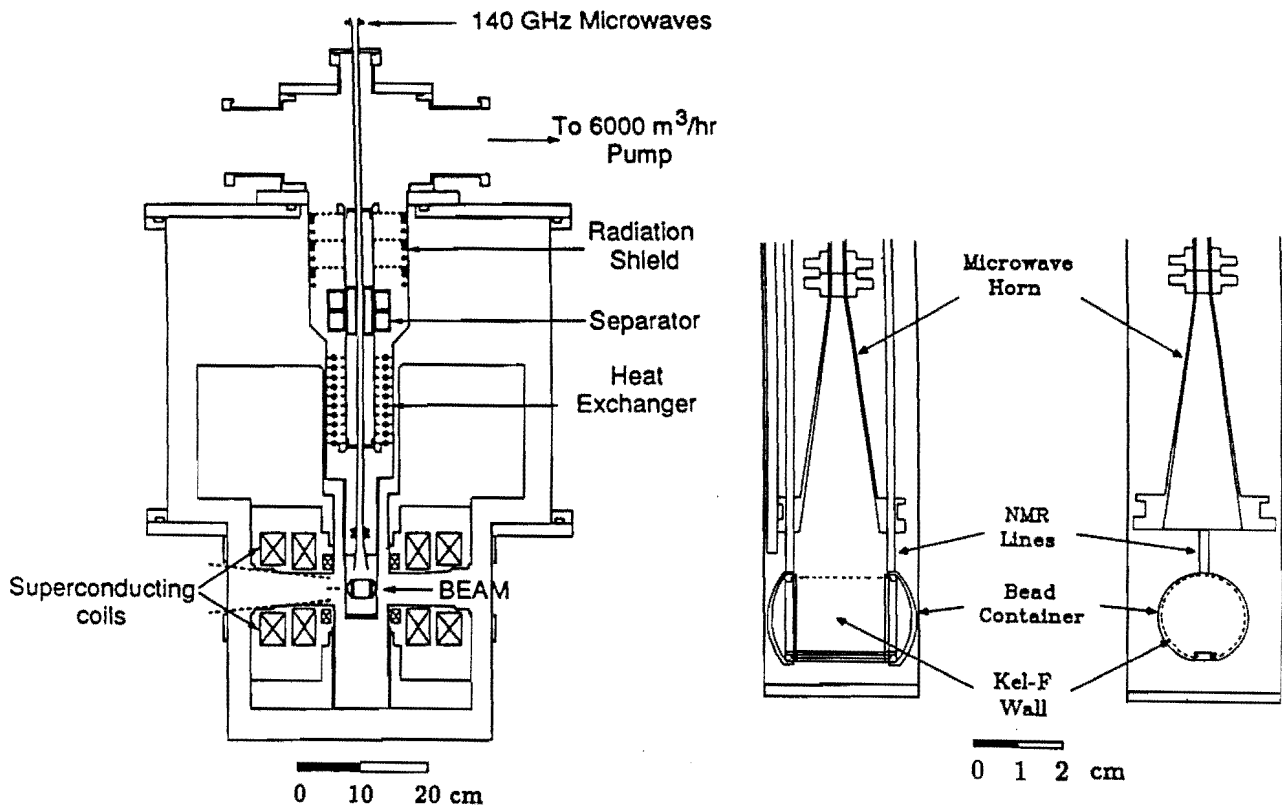


Figure 2. Diagram of the Michigan polarized proton target is shown on the left^[4]. The superconducting magnet produces a highly uniform 5 T field. At 1 K, the ^4He cryostat provides about 1 watt of cooling power to the irradiated NH_3 beads in the small target cavity, which is shown expanded on the right. The 140 GHz microwaves, from a 20 watt Varian EIO, are fed into the target cavity via the horn.

This target had an average polarization of 85% during a 3-month-long AGS run^[1] with an average beam intensity of about $2 \cdot 10^{11}$ protons per 2.4 sec AGS cycle. This was an average beam intensity of about 10^{11} protons per sec; it corresponds to almost $3 \cdot 10^{11}$ protons per 2.8 sec cycle at the Main Injector. Our experience at the AGS ^[1,4] suggests that there should be no problem caused by the slightly different cycle times of the AGS and the Main Injector.

The dilution factor decreases the true proton-proton elastic analyzing power due to the quasi-elastic and inelastic events from the heavy nuclei in the NH_3 beads, the He^4 and the container. The dilution factor was obtained at the AGS by measuring the event rate with hydrogen-free Teflon (CF_2) beads in place of ammonia beads and also from the off-diagonal matrix element coincidences between the forward and recoil hodoscopes. The measured dilution factor varied from about 1.06 at $P_{\perp}^2 = 3.2 \text{ (GeV/c)}^2$ to about 1.6 at $P_{\perp}^2 = 7 \text{ (GeV/c)}^2$ ^[1,30]. The dilution factor was rather close to one because the AGS double-arm elastic spectrometer strongly discriminated against quasi-elastic events and events from nitrogen and other heavy nuclei; the proposed SPIN@FERMI spectrometers should provide even better discrimination. However, the heavy nuclei would produce many inclusive events indistinguishable from the polarized protons' inclusive events ^[31]. Therefore, it would be very difficult to make inclusive measurements with this polarized target.

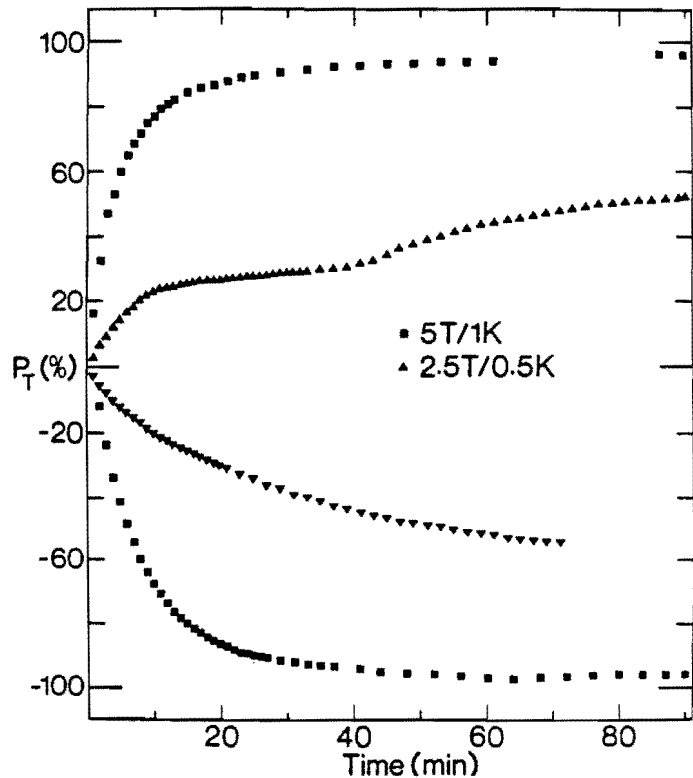


Fig. 3. The spin polarization of the free protons in NH_3 is plotted against the time of microwave irradiation. The target data at 5 T and 1 K are squares;^[4] the earlier NH_3 data at 2.5 T and 0.5 K are triangles.

1. Cryostat Temperature	1 K
2. Cooling Fluid	He^4
3. Cooling Power	0.93 watt
4. Operating Magnetic Field	5.0 T
5. Field Uniformity in 4 cm diam. by 3 cm high Region	10^{-4}
6. $\int B \cdot dl$	1.17 T · m
7. Power Supply Voltage	3 V
8. Superconducting Current	66 A
9. Microwave Frequency	≈ 140 GHz
10. NMR Frequency	(213.0 \pm 0.3) MHz
11. Vertical Angular Aperture	$\pm 6^\circ$
12. Horizontal Angular Aperture	$\pm 34^\circ$
13. Target Size	3.6 cm long by 2.0 cm diameter
14. Target Material	Irradiated NH_3 beads
15. Max. Average Beam Intensity	10^{11} sec $^{-1}$
16. Max. Polarization	96 %
17. Average Operated Polarization	85 %

Table 1. Michigan Solid PPT Specifications.

Rastering and Beam Stability Requirements

We propose to operate at the normal Main Injector energy of 120 GeV. Some proposed properties of the extracted beam at our PPT are:

1. Intensity: $3 \cdot 10^{11}$ protons per 2.8 sec pulse.
2. Beam spot size: 2.5 mm x 2.5 mm (HxV) FWHM.
3. Beam divergence: 0.05 mrad x 0.05 mrad (HxV) FWHM.

We wish to eliminate local overheating in our PPT, while still maintaining a small beam size to give precise vertex position identification. Therefore, we propose small upstream bending magnets to "raster" the beam across the area of our PPT during each 1 sec flat-top. This idea, which has been used at SLAC,^[32] is similar to the way electrons are swept across a TV screen. Our present plan is to have a 15 mm x 10 mm (HxV) effective beam size on our PPT by using 24 steps with a 2.5 mm x 2.5 mm instantaneous spot size as shown in Fig. 4.

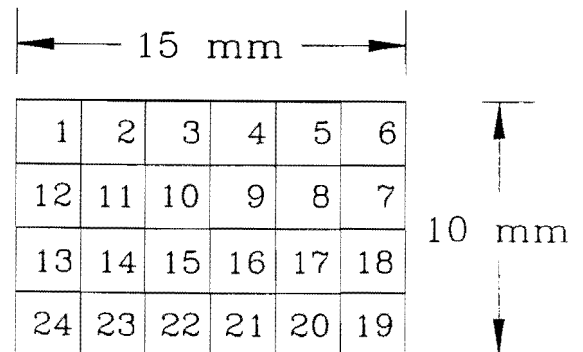


Fig. 4. Possible Raster Pattern

We propose to move the beam in this pattern using one set of horizontal and vertical dipole bending magnets placed about 30 m upstream of our PPT (MH_1 and MV_1) and a second set (MH_2 and MV_2) placed about 15 m upstream of the PPT as shown in Fig. 5. The maximum horizontal bending and vertical bending field integrals required would be $\int B \cdot dl = \pm 0.17 \text{ T}\cdot\text{m}$ and $\pm 0.10 \text{ T}\cdot\text{m}$, respectively. The first pair of rastering magnets would bend the beam by maximum horizontal and vertical angles of $\pm 0.417 \text{ mrad}$ and $\pm 0.250 \text{ mrad}$, respectively. The second magnet pair, with exactly equal but opposite $\int B \cdot dl$, would realign the beam's angle. With 24 raster positions in the total flattop time of about 1 second, one might spend 40 msec in each position and about 1.7 msec in each of the 23 moves.

The 120 GeV beam's intensity, position, and spot size must be very stable to provide reliable data and to avoid quenching the PPT's superconducting magnet. At the AGS,^[1,2,30] the average beam position was kept centered within $\pm 0.1 \text{ mm}$ despite the large variations in the D-line extracted beam's angle due to small energy variations; we used a servo system involving an upstream magnet with a fast response-time, controlled by the analog signal from the left-right asymmetry in a Segmented Wire Ion Chamber (SWIC) near the PPT. Fig. 5 shows a similar system at Fermilab which includes both position feedback and rastering. If the beam detected by the upstream horizontal and vertical split plate SWICS, S_{1H} and S_{1V} , is off-center, then appropriate currents would be applied to the rastering magnets to recenter and realign the "unrastered" beam onto the PPT. This centering system could be set up and periodically checked with the rastering off. Since the PPT magnet has an $\int B \cdot dl = 1.17 \text{ T}\cdot\text{m}$, another downstream magnet may be needed to realign the beam for possible downstream users or a beam dump.

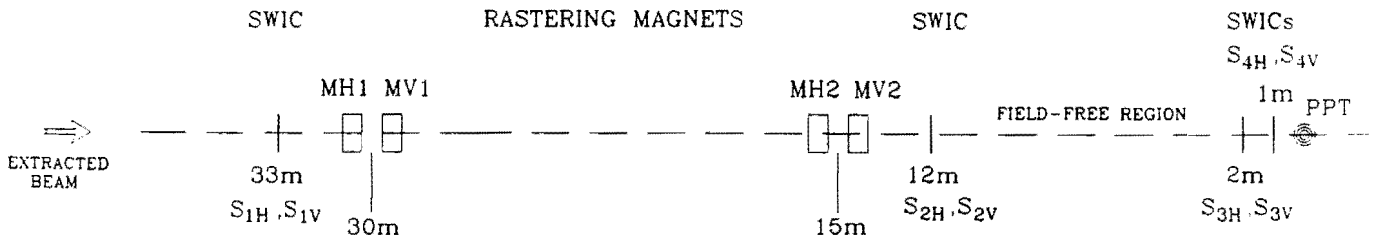


Figure 5. Possible beam-line system for rastering and centering the 120 GeV extracted beam at the PPT.

Recoil and Forward Spectrometers

Large- P_{\perp}^2 elastic events would be detected using a 40-m-long focusing recoil spectrometer, somewhat similar to that of our NEPTUN-A experiment, which may later study 400 GeV proton-proton elastic scattering at UNK in Protvino^[5]. The proposed SPIN@FERMI spectrometer is shown in Fig. 6. Table 2 lists, for each P_{\perp}^2 , the angle and momentum for both the forward and recoil proton, as well as the $\int B \cdot dl$ of each recoil-spectrometer magnet. Note that we considerably extend the spectrometer's range by reversing the PPT magnet for the large- P_{\perp}^2 points.

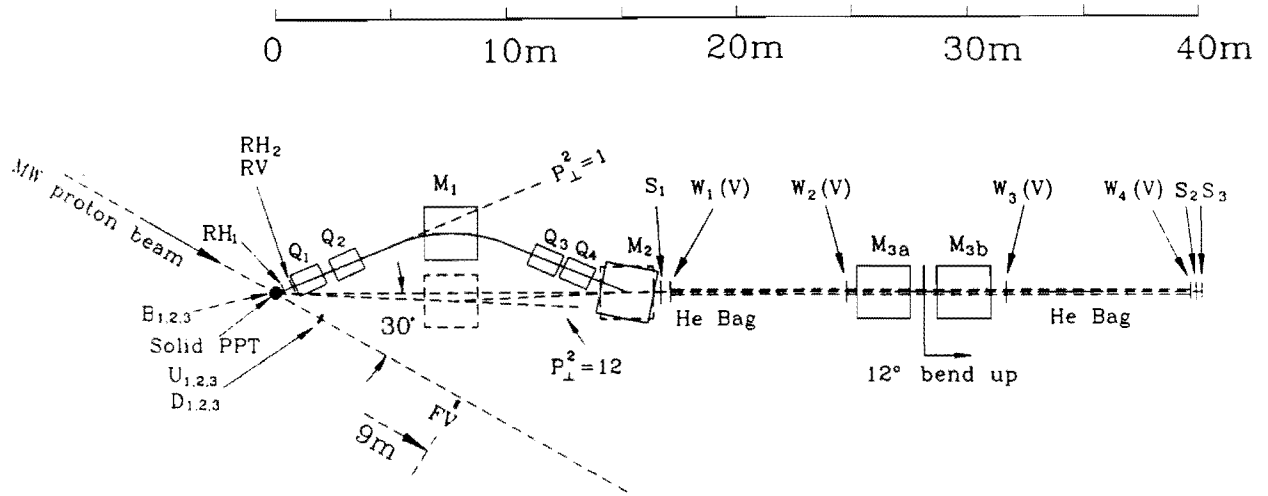


Fig. 6. Proposed 40-meter-long recoil spectrometer and simple forward spectrometer. The magnets and detectors are described in Tables 3, 4 and 6.

P_{\perp}^2 (GeV/c) ²	θ_F degrees	P_F GeV/c	θ_R degrees	P_R GeV/c	$\int Bdl_{PPT}^{eff}$ kG-m	θ'_R degrees	$\int Bdl_{M1}$ kG-m	$\int Bdl_{M2}$ kG-m	$\int Bdl_{M3a,M3b}$ kG-m
1	0.480°	119.5	61.65°	1.136	5.91	52.72°	29.3	-14.9	3.97
2	0.681°	118.9	52.53°	1.782	5.94	46.81°	34.4	-17.4	6.22
3	0.838°	118.4	46.68°	2.381	5.97	42.37°	34.0	-17.1	8.31
4	0.973°	117.8	42.43°	2.965	6.00	38.95°	30.8	-15.4	10.35
5	1.093°	117.3	39.13°	3.543	6.02	36.21°	25.6	-12.8	12.37
6	1.202°	116.7	36.47°	4.121	6.05	33.95°	18.9	-9.5	14.39
7	1.305°	116.1	34.25°	4.701	6.08	32.03°	11.1	-5.6	16.41
8	1.402°	115.6	32.37°	5.283	-6.11	34.35°	26.8	-13.4	18.45
9	1.495°	115.0	30.73°	5.870	-6.14	32.53°	17.3	-8.6	20.50
10	1.584°	114.4	29.30°	6.462	-6.17	30.94°	7.1	-3.5	22.56
11	1.670°	113.8	28.02°	7.059	-6.19	29.53°	-3.9	1.9	24.65
12	1.753°	113.2	26.88°	7.662	-6.22	28.28°	-15.4	7.7	26.75

Table 2. Angles and momenta of elastic protons and magnet strengths. Positive $\int Bdl$ denotes bending to the right for PPT, M_1 and M_2 and bending up for M_{3a} and M_{3b} . θ'_R is the recoil angle after the PPT magnet; it differs from θ_R by $\int Bdl_{PPT}^{eff}/P_R$.

The quadrupoles' gradients needed to focus the recoil protons into the spectrometer's apertures were calculated using TRANSPORT. Most focusing is done by the vertically focusing Q_1 and the horizontally focusing Q_2 ; this gives the spectrometer a larger vertical acceptance angle $\Delta\phi'_{lab} (= \Delta\phi \sin \theta_R)$ than horizontal acceptance angle $\Delta\theta_{lab}$. The horizontal angle θ_R is correlated with the elastic recoil momentum P_R for each P_{\perp}^2 . Fig. 7 shows typical horizontal (upper) and vertical (lower) beam envelopes through the spectrometer. The quadrupole pairs Q_1, Q_2 and Q_3, Q_4 focus a rather large acceptance of about $\Delta\theta_{lab} = 22$ mrad and $\Delta\phi'_{lab} = 140$ mrad into small aperture detectors and magnets. The required magnets are listed in Table 3.

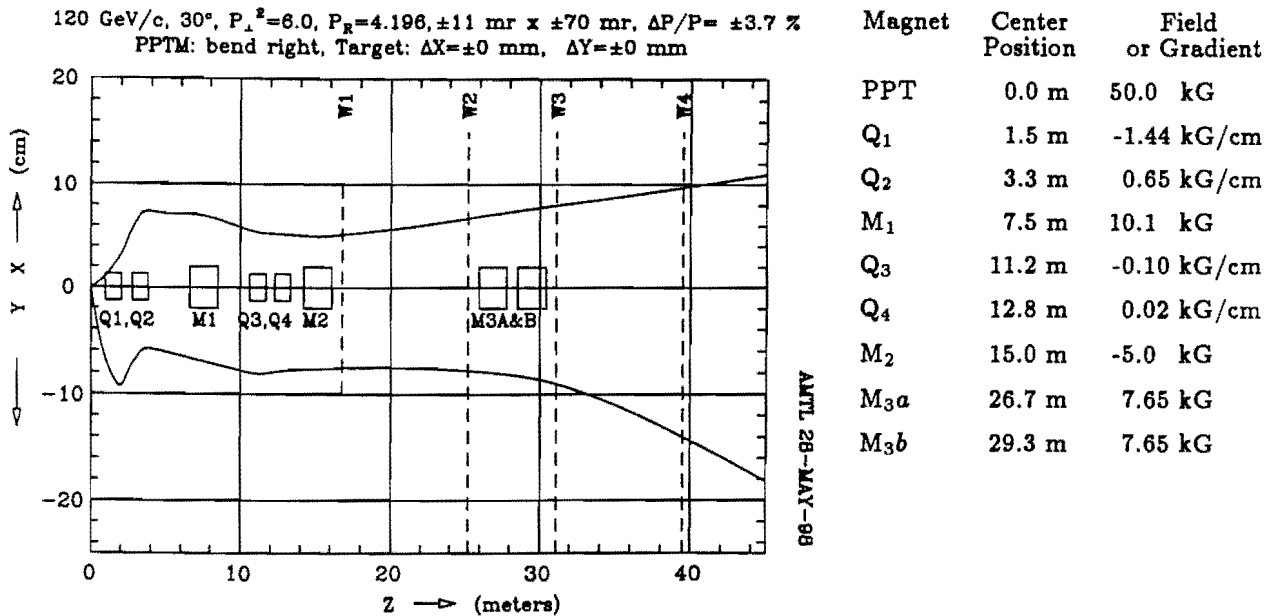


Figure 7. The beam envelopes obtained from TRANSPORT for the recoil protons at $P_{\perp}^2 = 6$ $(\text{GeV}/c)^2$ for a point target.

Magnet	Length (inches)	Gap (inches)	B'_{max} (kG/cm)	B_{max} (kG)
Q_1, Q_2, Q_3, Q_4	36	8x8	1.5	-
Q_1^{super}	24	4x6	6.0	-
M_1, M_2, M_{3a}, M_{3b}	72	24x8	-	18.5

Table 3. Recoil spectrometer magnet list.

We would probably later provide the superconducting quadrupole Q_1^{super} for the data runs at $P_{\perp}^2 = 7-12$ $(\text{GeV}/c)^2$; its field gradient of about 6 kG/cm, listed in Table 3, corresponds to the 7.7 GeV/c recoil momentum at $P_{\perp}^2 = 12$ $(\text{GeV}/c)^2$; the corresponding beam envelope plot is shown in Fig. 8. The Q_1^{super} aperture is 4 x 6 inches and its center is 30 cm closer to the target than Q_1 .

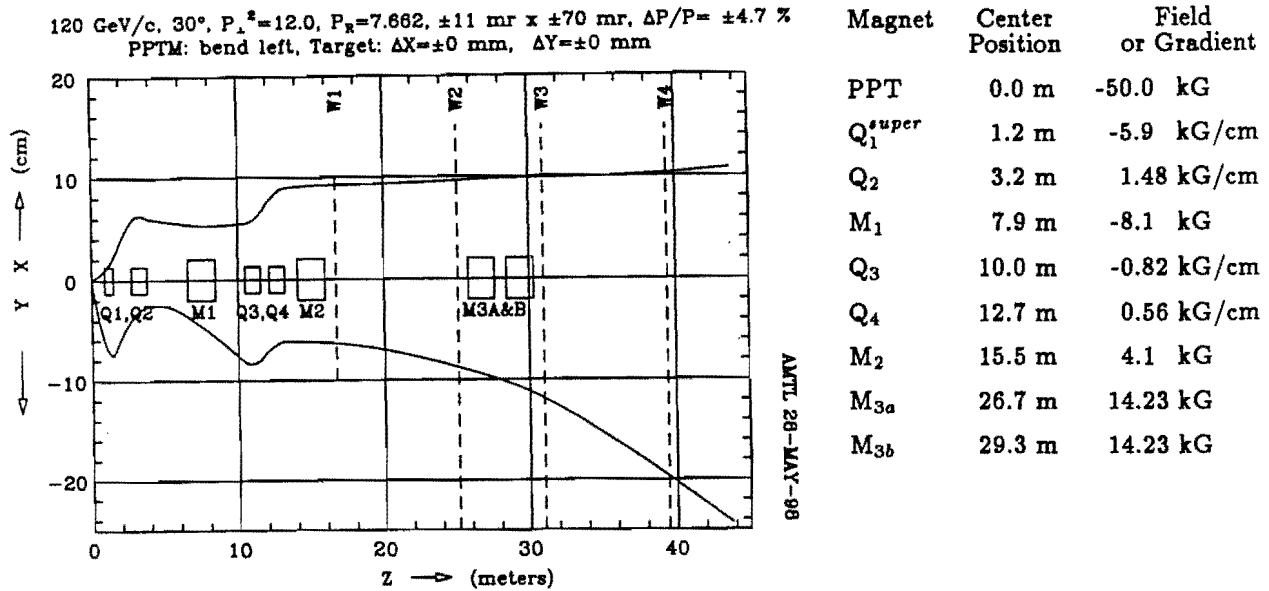


Figure 8. Beam envelope plot for the highest $P_L^2 = 12 \text{ (GeV/c)}^2$. Q_1^{super} should be a superconducting quadrupole with a gradient of about 6 kG/cm for $P_L^2 = 7-12 \text{ (GeV/c)}^2$.

As shown in Figs. 6 and 9, the forward arm would contain a small vertical resolution hodoscope FV. Table 4 lists the sizes of all detectors. The 12° vertical bend in the M_3 dipole, measured with the 1 mm vertical resolution wire chambers W_1 to W_4 , would give a momentum resolution of about $\pm 0.1\%$. The scintillator hodoscopes RH_1 and RH_2 would measure the horizontal recoil angle θ_R with a precision of approximately $\Delta\theta_R \approx \pm\sqrt{(0.28)^2 + (0.35)^2}/50 = \pm 8.8 \text{ mrad}$.

By recording each event's time-step during the 24-step 1 sec raster, we would determine the transverse position of the interaction point to a precision of 2.5 mm FWHM. This would determine the vertical forward angle (ϕ'_F) and vertical recoil angle (ϕ'_R) to precisions of approximately:

$$\Delta\phi'_F \approx \pm\sqrt{(2.5)^2 + (2.3)^2} \text{ mm}/9\text{m} = \pm 0.38 \text{ mrad},$$

$$\Delta\phi'_R \approx \pm\sqrt{(2.5)^2 + (4.4)^2} \text{ mm}/0.8\text{m} = \pm 6.3 \text{ mrad}.$$

This would determine coplanarity to a precision of about $\Delta\phi = \pm 14 \text{ mrad}$ at 6 (GeV/c)^2 which would significantly discriminate against inelastic and quasi-elastic events. The $\pm 0.1\%$ P_R measurement and the $\pm 8.8 \text{ mrad}$ measurement of θ_R would even more strongly discriminate against background events. We would monitor the relative luminosity using the U_{123} , D_{123} , and B_{123} telescopes, of 3 small scintillation counters each, placed above and below the beam line.

We would employ a three-level system to select elastic events. The first level would be a fast coincidence (S_{123}) between the scintillator hodoscopes S_1 , S_2 and S_3 ; its decision time would be about 5 nsec. S_1 , S_2 and S_3 would each have 4 hodoscope channels, which would give a momentum resolution of about $\Delta P/P = \pm 5\%$. The second level trigger would include an "or" coincidence with any FV hodoscope channel ($S_{123} \cdot FV_{or}$). This would have the same decision time of about 5 nsec

and would give a fast and simple estimate of the elastic event rate. However, it would probably have a high background rate at high- P_{\perp}^2 and a high accidental rate at low- P_{\perp}^2 .

Detector	Type	Location	Size(HxV) [cm]	Channels	Resolution [cm]	Other specifications
S ₁	Scintillator	R-16.6 m	20x20	4	5 V	5 mm thick
S ₂	Scintillator	R-39.7 m	30x50	4	12.5 V	1 cm thick
S ₃	Scintillator	R-40.0 m	30x50	4	12.5 V	1 cm thick
RH ₁	Scintillator	R-0.3 m	4.5x6.2	16	0.28 H	5 mm thick
RH ₂	Scintillator	R-0.8 m	5.6x13.2	16	0.35 H	5 mm thick
RV	Scintillator	R-0.8 m	5.6x13.2	32	0.41 V	5 mm thick
W ₁	MWPC	R-16.7 m	20x20	192	0.1 V	
W ₂	Drift Chamber	R-25.1 m	30x50	2x32	0.1 V	Ar-CO ₂
W ₃	Drift Chamber	R-31.0 m	30x50	2x32	0.1 V	Ar-CO ₂
W ₄	Drift Chamber	R-39.4 m	30x50	2x32	0.1 V	Ar-CO ₂
FV	Scintillator	F-9 m	3x7.5*	32	0.23 V*	2.54 cm thick
U ₁₂₃	Scintillators	F-2 m, 20° up	1.27x1.27	3	–	2.54 cm thick
D ₁₂₃	Scintillators	F-2 m, 20° down	1.27x1.27	3	–	2.54 cm thick
B ₁₂₃	Scintillators	1 m below	1.0x2.0	3	–	0.5 cm thick

* These are the matched FV sizes for $P_{\perp}^2 = 6$ (GeV/c)²; we would use different size scintillators at larger and smaller P_{\perp}^2 to match the elastic kinematics.

Table 4. List of detectors.

Each second level trigger would be analysed by two independent on-line data analysis systems: a fast hard-wired system and a slower computer system for more detailed analysis.

The fast hard-wired system would require a coincidence between the recoil and forward ϕ angles measured by the 32 channel recoil hodoscope RV and the 32 channel forward hodoscope FV. Adjacent channels would be grouped to form an 8 x 8 coplanarity coincidence matrix using a memory look-up unit (MLU) with a decision time of about 50 nsec; a negative decision would clear all subsystems to decrease the dead time. The “off-diagonal” 8 x 8 matrix elements would be used for a fast estimate of the background. Time-to-digital converters (TDCs) would record the time-of-flight between S₁ and S₃ and estimate the accidental coincidences between FV and RV.

All (32 x 32) channels would be individually analysed by the computer system. For each event, the computer system would also form an angle-momentum cut by correlating the horizontal recoil angle measured by the 16 channel RH₁ and RH₂ hodoscopes with the precise momentum measurement from the four wire chambers W₁ to W₄. This computer analysis should take at most a few milliseconds; thus, it might be off-line for a significant fraction of the small- P_{\perp}^2 events, but it certainly would be on-line for almost all large- P_{\perp}^2 events.

Note that the most serious problem may be the very high rates in the RH_1 and FV scintillation hodoscopes. With the total NH_3 luminosity of over $10^{35} \text{ cm}^{-2} \text{ s}^{-1}$ at Main Injector, each channel may run at several MHz as did similar detectors at the AGS^[1,30]. We would use a separate power supply for each dynode in both RH_1 and FV and also use thick scintillators and low PM tube voltages in FV.^[30]

We propose installing the spectrometers and the polarized proton target (PPT) in the Meson West extracted beam line, as shown in Fig. 9. The SPIN Collaboration would provide all detectors, electronics, and data analysis computers. The following modifications of the Meson West area would be required:

1. Rearrangement of shielding blocks and possibly raising the roof shielding to accommodate the PPT with its pumps and cryogenic hardware.
2. Rearrangement of the area around the 30° spectrometer line to accommodate the detectors and downstream magnets.

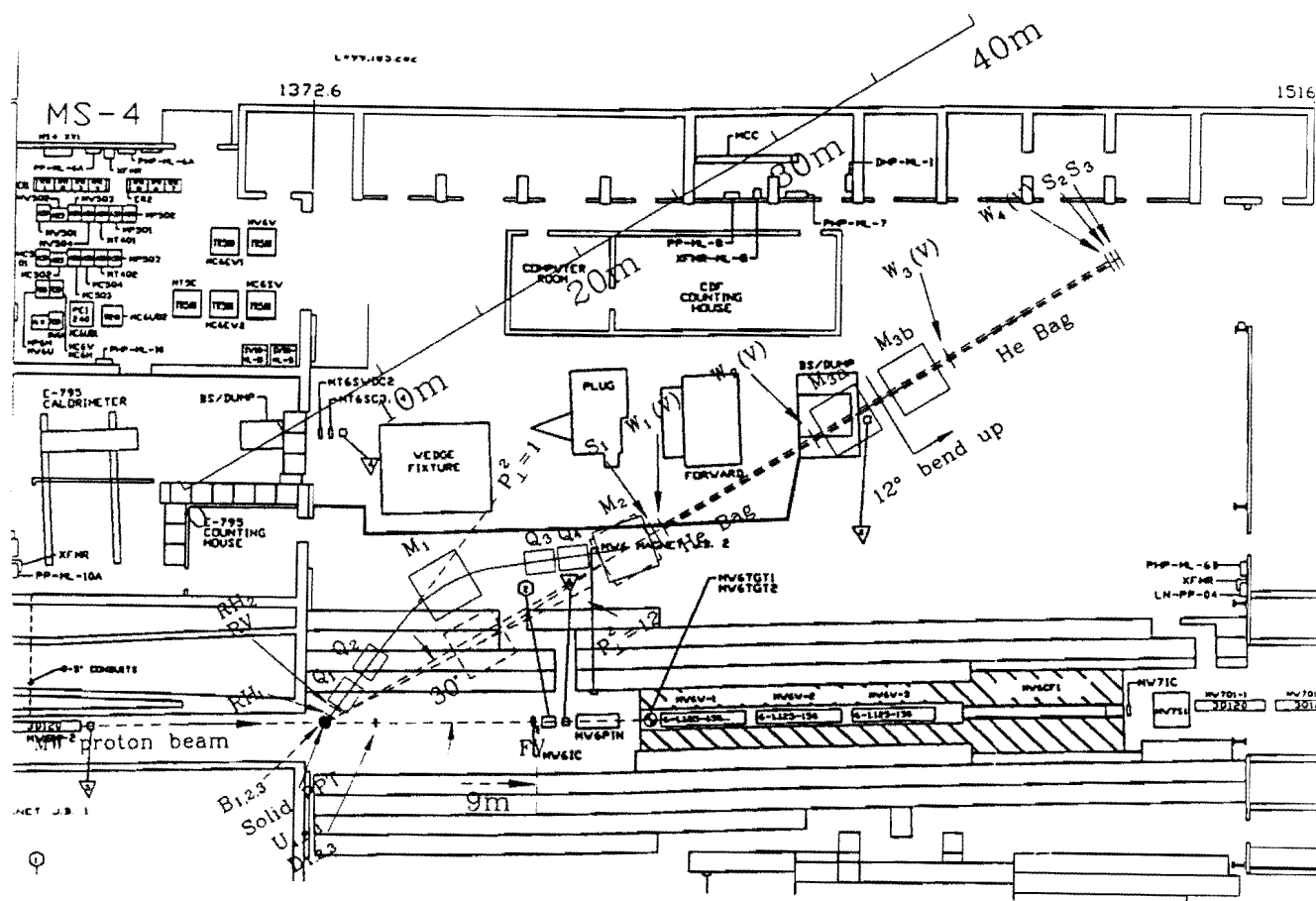


Figure 9. Possible SPIN@FERMI layout of the PPT and the forward and recoil spectrometers in the Meson West area.

Event Rates

We estimate the event rates and errors in A_n for large- P_{\perp}^2 proton-proton elastic scattering at 120 GeV using the Michigan polarized target and the proposed SPIN@FERMI spectrometers. Our target has a polarized proton thickness of about:

$$N_0(\rho)t = 6.02 \cdot 10^{23} \text{ gm}^{-1} (0.1 \text{ gm cm}^{-3}) 3.6 \text{ cm} = 2.1 \cdot 10^{23} \text{ polarized protons cm}^{-2}. \quad (4)$$

The Main Injector can easily supply $3 \cdot 10^{11}$ unpolarized 120 GeV protons with a 2.8 sec repetition rate to the Meson West area. Then the average intensity passing through our target would be about 10^{11} protons per sec; the time-averaged luminosity would then be:

$$\mathcal{L} = 2.1 \cdot 10^{34} \text{ sec}^{-1} \text{ cm}^{-2}. \quad (5)$$

The $p-p$ elastic cross-sections, $d\sigma/dt$, are obtained from a compilation^[33] shown in Fig. 10; at 120 GeV/c, $\beta_{cm} = 0.9922$ and $\sigma_{total} = 38.5 \text{ mb}$, so that the quantity $\beta^2 \sigma_{total}/38.3 = 0.990$, which is quite close to 1. We then calculate the event rate using:

$$\text{Events/day} = \mathcal{L} \frac{d\sigma}{dt} (\Delta t \cdot \Delta\phi/2\pi) \epsilon \cdot 86400 \text{ sec/day} = 144 \frac{d\sigma}{dt} [\text{nb}] \Delta t \cdot \Delta\phi [\text{mr}], \quad (6)$$

where $\Delta\phi$ is the azimuthal angle and the detection efficiency ϵ is conservatively estimated to be 50 %. Table 5 lists the event rate and error in A_n for each P_{\perp}^2 point. Note that we may need a lower beam intensity at $P_{\perp}^2 = 1 \text{ (GeV/c)}^2$. As an example of what might be done with a 70 % polarized Main Injector beam, we also list ΔA_{nn} , the elastic spin-spin parameter's error.

P_{\perp}^2 (GeV/c) ²	Δt (GeV/c) ²	$\Delta\phi$ mr	$d\sigma/dt$ $\frac{\text{nb}}{(\text{GeV/c})^2}$	<u>events</u> day	days	N events	ΔA_n [.85 \sqrt{N}] ⁻¹	ΔA_{nn} [.70(.85) \sqrt{N}] ⁻¹
1.0	0.06	159	2200	3.03 10 ⁶	5	1.52 10 ⁷	0.1%	0.1%
2.0	0.09	177	70	1.61 10 ⁵	5	8.06 10 ⁵	0.2%	0.2%
3.0	0.25	194	16	1.12 10 ⁵	5	5.60 10 ⁵	0.2%	0.3%
4.0	0.35	210	3.1	3.29 10 ⁴	5	1.64 10 ⁵	0.3%	0.4%
5.0	0.45	225	0.73	1.07 10 ⁴	5	5.34 10 ⁴	0.5%	0.8%
6.0	0.56	240	0.16	3.10 10 ³	10	3.10 10 ⁴	0.7%	1.0%
7.0	0.67	254	0.039	960	15	1.44 10 ⁴	1.0%	1.4%
8.0	0.79	268	0.009	276	20	5.51 10 ³	1.6%	2.3%
10.0	1.06	296	0.0014	64	30	1.90 10 ³	2.7%	3.9%
12.0	1.25	324	0.00021	12	50	6.14 10 ²	4.8%	6.8%
Total					150 days+15 days tune-up			

Table 5. Event rates and errors in A_n and A_{nn} for $p-p$ elastic scattering at 120 GeV/c. The high- P_{\perp}^2 points below the dotted line require Q_1^{super} .

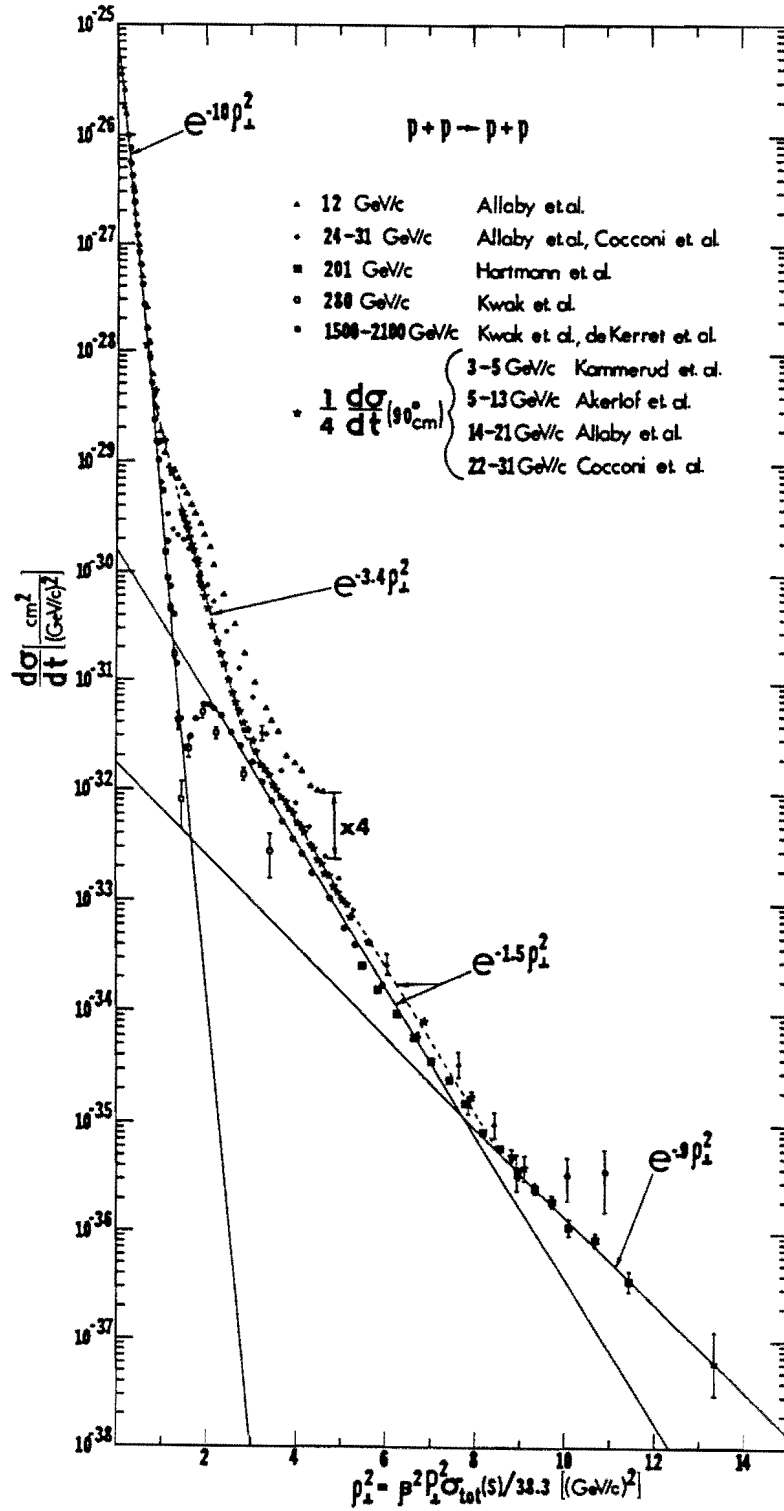


Figure 10. The $p - p$ elastic cross-sections plotted against the variable ρ_1^2 . [33]

Status of Equipment

Table 6 lists the status of the equipment required for the SPIN@FERMI experiment. Significant time would be required for the careful packing, shipping, and reassembling of the solid PPT system now at Michigan. This summer, we again successfully tested this solid PPT at Michigan; in 1996, with freshly irradiated ammonia beads, a polarization of over 90% was obtained.

#	Item	Status	Suggested action	Estimated time
1.	Solid PPT, NMR, Microwaves	At Michigan	Pack, ship, reassemble	6 months
2.	PPT pumps	At Michigan	Pack, ship, reassemble	6 months
3.	PPT stand + hardware	At Michigan	Modify and ship	3 months
4.	Quadrupoles Q1, Q2, Q3, Q4	From FNAL	Find	3 months
5.	Dipoles M1, M2, M3 _a , M3 _b	From FNAL	Find	3 months
6.	Movable stands for: Q1,Q2,Q3,Q4 M1,M2,M3 _a ,M3 _b	Need	Make at FNAL	3 months
7.	Magnets' movement plates	Need	Design, make at FNAL	6 months
8.	Magnets' power supplies	From FNAL	Obtain, check	3 months
9.	Scintillators: FV,S1,S2,S3,RH2,RH2,RV	Need	Make at Michigan	4 months
10.	Wire Chambers: W1,W2 W3,W4	At Michigan Need	Pack, ship Make at Michigan	2 months 6 months
11.	Monitors D ₁₂₃ , U ₁₂₃ , B ₁₂₃	At Michigan	Check, ship	3 months
12.	Detector stands	At Michigan	Pack, ship	3 months
13.	Cables Connectors Connect cable ends	Need Mostly at Michigan Need	Purchase Acquire, ship Assemble, test at Michigan	2 months 3 months 2 months
14.	Electronics	Mostly at Michigan	Acquire, ship	3 months
15.	Computers	At Michigan	Pack, ship	2 months
16.	SWIC's	From FNAL	Check, install in beam line	2 months
17.	Feedback split SWICs	Need	Build at FNAL or Michigan	4 months
18.	Rastering & stability: magnets, power supplies and controls	From FNAL	Design	6 months
19.	Experiment's trailer	From FNAL	Obtain, modify	3 months
20.	Shielding blocks	At FNAL	Plan, rearrange	3 months
21.	Liquid Helium and Nitrogen	Through FNAL	Purchase, reliquify	1 month
22.	Superconducting Q1	Will need later	Design, purchase or fabricate	18 months

Table 6. Status of equipment

Summary

We propose fundamental measurements of the analyzing power A_n in 120 GeV $p-p$ elastic scattering at high- P_{\perp}^2 , which should give important information and insights about the inner structure of the proton and the strong interaction. We should be able to precisely measure A_n from $P_{\perp}^2 = 1$ to $12 (\text{GeV}/c)^2$ in 150 days of data time plus about 15 days of tune-up time. The SPIN@FERMI experiment would utilize the proven Michigan solid polarized proton target and the carefully studied design of the NEPTUN-A spectrometer. This proposed experiment would increase the maximum measured P_{\perp}^2 for A_n data from 7 to $12 (\text{GeV}/c)^2$ and would increase the maximum energy for large- P_{\perp}^2 A_n data from 28 to 120 GeV.

References

- [1] D. G. Crabb *et al.*, Phys. Rev. Lett. **65**, 3241 (1990).
- [2] P. R. Cameron *et al.*, Phys. Rev. Rap. Comm. **D32**, 3070 (1985);
D. C. Peaslee *et al.*, Phys. Rev. Lett. **51**, 2359 (1983);
P. H. Hansen *et al.*, Phys. Rev. Lett. **50**, 802 (1983).
- [3] J. Antille *et al.*, Nucl. Phys. **B185**, 1 (1981).
- [4] D. G. Crabb *et al.*, Phys. Rev. Lett. **64**, 2627 (1990).
- [5] A. D. Krisch, in *Proceedings of the Workshop on UNK*, ed. N. E. Tyurin, 152 (Protvino, Russia 1989).
- [6] G. P. Lepage and S. J. Brodsky, Phys. Rev. **D22**, 2157 (1980).
- [7] S. J. Brodsky and G. Farrar, Phys. Rev. Lett. **31**, 1153 (1973);
V. A. Matveev, R. M. Muradyan and A. N. Tavkhelidze, Lett. Nuovo Cimento **7**, 719 (1973).
- [8] A. D. Krisch, *the 9th International Symposium on High Energy Spin Physics*, Bonn, 1990, Springer-Verlag **1**, 57 (1991); Summary of the *11th International Symposium on High Energy Spin Physics*, Indiana, 1994, A.I.P. Conf. Proc. **343**, 3 (1995).
- [9] S. M. Troshin and N. E. Tyurin, Int. J. Modern Phys. **A5**, 2689 (1990); *Spin Phenomena in Particle Interactions*, World Scientific (1994), and references listed therein.
- [10] T. Gousset, B. Pire, J. P. Ralston, Phys. Rev. **D53**, 1202 (1996).
- [11] J. R. O'Fallon *et al.*, Phys. Rev. Lett. **39**, 733 (1977);
D. G. Crabb *et al.*, Phys. Rev. Lett. **41**, 1257 (1978).
- [12] E. A. Crosbie *et al.*, Phys. Rev. **D23**, 600 (1981);
A. Lin *et al.*, Phys. Lett. **74B**, 273 (1978).
- [13] D. L. Adams *et al.*, Phys. Lett. **B276**, 531 (1992).

- [14] K. J. Heller *et al.*, Phys. Rev. Lett. **41**, 607 (1978).
- [15] G. R. Farrar *et al.*, Phys. Rev. **D20**, 202 (1979).
- [16] S. J. Brodsky, C. E. Carlson and H. J. Lipkin, Phys. Rev. **D20**, 2278 (1979).
- [17] A. W. Hendry, Phys. Rev. **D23**, 2075 (1981).
- [18] S. J. Brodsky and G. F. de Teramond, Phys. Rev. Lett. **60**, 1924 (1988).
- [19] S. M. Troshin and N. E. Tyurin, J. Phys. (Paris), Colloq. **46**, C2-235 (1985).
- [20] G. Nardulli, G. Preparata, J. Soffer, Nuovo Cimento **83A**, 361 (1984); Phys. Rev. **D31**, 626 (1985).
- [21] B. Pire and J. Ralston, AIP Conf. Proc. **95**, 347 (1983).
- [22] C. Avilez, G. Cocho and M. Moreno, Phys. Rev. **D24**, 634 (1981).
- [23] M. Anselmino, P. Kroll and B. Pire, Z. Phys. **36**, 89 (1987).
- [24] S. V. Goloskokov, S. P. Kuleshov and O. V. Seljugin, in *Proc. of the 7th International Symposium on High Energy Spin Physics*, Protvino (1986).
- [25] P. A. Kazaks and D. L. Tucker, Phys. Rev. **D37**, 222 (1988).
- [26] H. J. Lipkin, Nature (London) **324**, 14 (1986); Phys. Lett. **B181**, 164 (1986).
- [27] C. E. Bourrely *et al.*, Phys. Rep. **177**, 319 (1989).
- [28] D. G. Crabb *et al.*, Phys. Rev. Lett. **60**, 2351 (1988);
F. Z. Khiari *et al.*, Phys. Rev. **D39**, 45 (1989).
- [29] S. M. Troshin, *Private communication* (1998).
- [30] J. A. Stewart, *The analyzing power in 24 GeV/c proton-proton elastic scattering at $P_{\perp}^2 = 3.2$ to 7.1 (GeV/c)²*, University of Michigan thesis (1992).
- [31] T. Shima, *Spin asymmetries in inclusive cross sections*, University of Michigan thesis (1981).
- [32] D. G. Crabb, *Private communication* (1998).
- [33] A. D. Krisch, Z. Phys. C - Particles and Fields **46**, 3241 (1990); Phys. Rev. Lett. **19**, 1149 (1967).